Int. J. Microgravity Sci. Appl. 33 (2) 2016,330213
DOI: 10.15011/ijmsa.33. 330213

IIIII ISPS-6 Proceedings IIIII
(Original Paper)

SiGe Crystal Growth by the Traveling Liquidus-Zone Method aboard the International Space Station

Kyoichi KINOSHITA[1], Yasutomo ARAI[1], Yuko INATOMI[1], Takao TSUKADA[2], Hiroaki MIYATA[3], Ryota TANAKA[3], Keita ABE[2], Sara SUMIOKA[2], Masaki KUBO[2] and Satoshi BABA[2]

Abstract

Total of four SiGe crystal growth experiments aboard the ISS were successfully performed for evaluating a two-dimensional growth model of the traveling liquidus zone (TLZ) method and for obtaining insights into large homogeneous SiGe crystal growth conditions. The TLZ growth requires diffusion limited mass transport in a melt and experiments in microgravity are essential. Although a little deviation from the expected compositional uniformity due to emissivity change of the cartridge surface is observed, homogeneous SiGe crystals are grown. Over all axial growth rate is consistent with the one-dimensional TLZ growth model prediction. However, radial growth rates are different from the two-dimensional growth model prediction. The difference is closely related to the flat interface shape in space grown crystals compared with the terrestrial ones and the radial compositional uniformity is much better than those of terrestrially grown crystals. Suppression of convection in a melt is favorable for obtaining flat freezing interface and is beneficial to large homogeneous SiGe crystal growth. It is expected that the obtained results are utilized and large homogeneous crystal growth is realized on the ground and electronic devices using SiGe substrates are developed.

Keyword(s): SiGe, crystal growth, TLZ method, ISS, Microgravity

Received 12 September 2015, Accepted 30 December 2016, Published 30 April 2016

1. Introduction

Mix crystals between Si and Ge (abbreviated as SiGe) are possible for any ratios of Si/Ge and are promising for substrates of electronic devices. High electron mobility for Si thin films and high hole mobility for Ge thin films both epitaxially grown on SiGe substrates are expected by the induced strain in thin films due to lattice mismatch between films and SiGe substrates. However, growth of bulk homogeneous SiGe crystals is very difficult due to large separation of liquidus and solidus lines in the phase diagram of the Si-Ge system[1,2)]. For growing homogeneous bulk mixed crystals we invented a new growth method named as a traveling liquidus zone (TLZ) method[3)]. This method is a kind of zone melting method but is different from the conventional zone melting method in the formation of saturated solution zone (liquidus zone)[3)]. The TLZ method requires diffusion limited mass transport in a liquidus zone and theoretically analyzed growth rates were compared with those of small diameter TLZ-grown crystals and it is shown that the proposed one-dimensional TLZ growth model agreed well with experiments[4)]. For fabricating substrates large diameter crystals are required and a two-dimensional TLZ growth model was proposed[5)] but this model could not be evaluated on the ground due to occurrence of convection in a large diameter liquidus zone[6)] and crystal growth experiments in microgravity were proposed[7)].

Total of four SiGe crystal growth experiments aboard the "Kibo" in the ISS were carried out. The first experiment was carried out in 2013 for checking thermal conditions in a sample in microgravity because suppression of convection in a melt zone affected the temperature profile in a space processed sample[8)]. The second and the third experiment were performed at growth rates around 0.1 mm/h[9,10)]. Growth length in the third experiment was 1.5 times as long as that of the second one. The last (fourth) experiment was performed in July 2014 at a higher temperature gradient compared with the second and the third one. In this paper, we report on a brief summary of four experiments.

2. Experiments

Crystal growth experiments for aiming at $Si_{0.5}Ge_{0.5}$ homogeneous composition were carried out by the TLZ method using a gradient heating furnace (GHF) installed in the "Kibo" (the Japanese Experiment Module, JEM). Experimental details were published elsewhere[8)]. Here, they are briefly described. Diameter of a grown crystal was 10 mm and the growth length was between 10 and 17 mm. Zone forming material Ge was

1 Japan Aerospace Exploration Agency, 2-1-1, Sengen, Tsukuba, Ibaraki 305-8505, Japan.
2 Deprtment of Chemical Engineering, Tohoku University, 6-6-07, Aramaki, Aoba-ku, Sendai 980-8579, Japan.
3 Advanced Engineering Services Co. Ltd, 1-6-1, Takezono, Tsukuba, Ibaraki 305-0032, Japan.
(E-mail: kinoswhita.kyoichi@jaxa.jp)

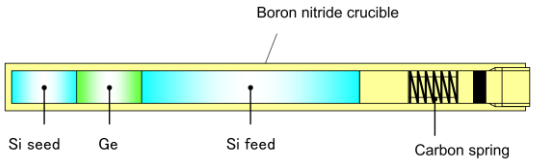

Fig. 1 Cross sectional view of a sample set up.

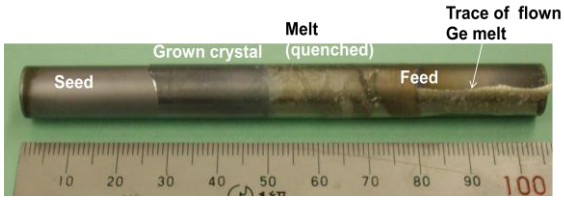

Fig. 2 Outer view of a space-processed sample.

sandwiched between the Si seed and the Si feed in a boron nitride crucible as shown in **Fig. 1**. The crucible was vacuum sealed in a quartz ampoule. The ampoule was set in a metal cartridge and inserted into the GHF. By heating the cartridge at around 1200 °C, lower melting temperature Ge was melted while Si was solid and a Ge rich liquidus zone was formed. By imposing a constant temperature gradient in the axial direction, the SiGe crystal was grown due to the inter diffusion between Si and Ge in the liquidus zone. The temperature gradient at the freezing interface was set at 9 °C/cm for the first to the third experiment and 18 °C/cm for the fourth experiment. Temperature profiles in the cartridge were controlled by three zone heaters in the GHF. Heater temperatures were controlled by a programmed temperature-time sequence. In the third experiment, heater temperatures were adjusted by commands from the operation center on the ground. Step temperature change of 1°C for every adjustment was applied. Orientation of the Si seed was <100>. For avoiding the free melt surface, the Si feed was pushed towards the melt by a carbon spring in a crucible as shown in **Fig. 1**.

Grown crystals were returned back to the ground using the Space-X or the Soyuz. They were cut parallel to the growth axis by a wire cutter and the surface of the cross section was polished. Si and Ge composition distribution of the polished surface was analyzed by an electron probe micro analyzer (EPMA). Crystallographic orientation was analyzed by the electron backscatter diffraction (EBSD).

3. Results and Discussion

3.1 Outer View of a Space-Grown Crystal

An example of the outer view of a space-grown crystal is shown in **Fig. 2**. No missing part and major cracks were observed. Traces of flown melt on the feed surface showed no free melt surface during crystal growth. The seed part, the grown crystal part, the quenched liquidus-zone part, and the feed part can be distinguished by reflected color difference. A single crystal was grown on a Si seed in spite of the lattice mismatch of about 2 % between Si and $Si_{0.5}Ge_{0.5}$ because lattice parameter of Si is 0.543 nm and that of $Si_{0.5}Ge_{0.5}$ is 0.554 nm. Although the lattice mismatch induced many dislocations at the seed crystal interface, the number of dislocations decreased as crystal growth proceeded. The length of the single crystal was about 5 mm and the total length of the grown crystal was about 17 mm. Polycrystallization at about 5 mm growth position may not be due to lattice mismatch but due to the constitutional supercooling. Origins of polycrystallization are now being analyzed.

3.2 Axial Compositional profile

Measured axial compositional profiles of the first space-grown crystal are shown in **Fig. 3**. Obtained profiles show Ge concentration of 48.5 plus or minus 2 at.%, for the growth length of 17.2 mm which are consistent with the predicted ones by the one-dimensional TLZ growth model[4] except for small unexpected deviation as pointed out by an arrow. Such deviation

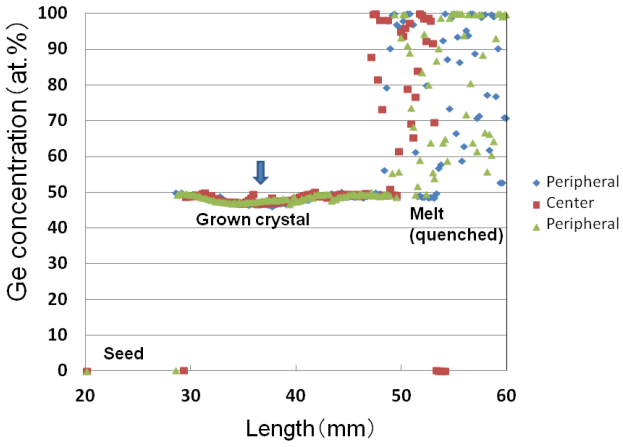

Fig. 3 Axial Ge concentration profiles of a space-grown crystal compared with a center line and two peripheral regions.

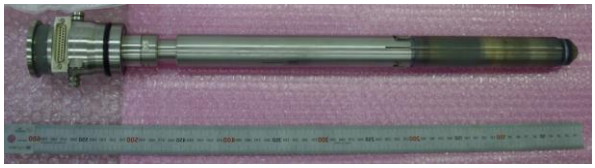

Fig. 4 Outer view of a space-processed cartridge. The brown part is a heated part.

was caused by the emissivity change of the surface of the cartridge as revealed by the numerical simulation[11]. Outer view of the returned cartridge of this sample is shown in **Fig. 4**. The cartridge was heated up to 1250 °C in vacuum condition of about 10^{-3} Pa during crystal growth and the heated part was color-changed from metallic luster to brown as shown in **Fig. 4**. It was thought that the color-change induced emissivity change and resulted in its inside temperature change even if heater temperatures were controlled constant. The numerical simulation of temperature profiles in the sample based on measured temperatures using 5 thermocouples attached on the cartridge surface was performed and compositional analyses based on the simulated temperature profiles were also performed and such compositional deviation was confirmed[11].

3.3 Radial Compositional Uniformity

Radial compositional uniformity was excellent compared with terrestrially grown crystals[9, 10]. An example of the radial compositional profile is shown in **Fig. 5**. This result was obtained for the third sample and such uniform composition was obtained for the growth length between 3 to 9 mm. The total growth length was about 15 mm and excellent radial compositional uniformity was established for about 40 % of the grown crystal. Such radial compositional uniformity is closely related to the freezing interface shape. Comparing with the terrestrially grown crystal, the interface shape is rather flat as discussed later in more detail, and the flat interface may contribute to the excellent uniformity.

3.4 Interface Curvature

In the third crystal, striations (white lines) are observed by a backscattered electron image as shown in **Fig. 6**. Since the number of heater temperature change coincided with the number of striations, it is concluded that these striations were formed by step temperature change during crystal growth. The slight concentration difference of about 0.2 at % in Ge caused by 1 °C temperature change gave such graded effect in the observed image. Detailed analysis of compositional variation along and

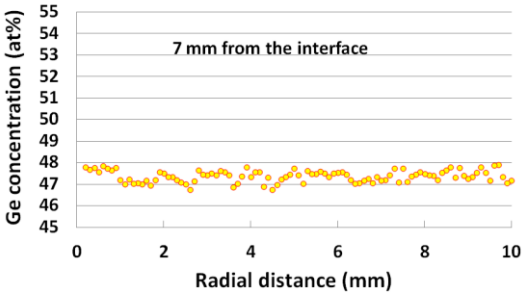

Fig. 5 An example of the radial compositional profile.

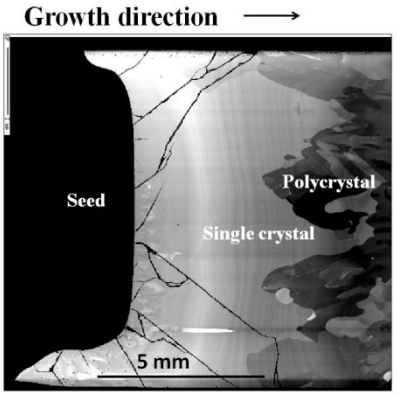

Fig. 6 Backscattered electron image of a space processed sample. Striations caused by a stepwise heater temperature change were observed.

across striations and growth rate determination using the relation between spacing of striations and temperature change intervals will be published elsewhere[12], but very briefly it can be said that the growth interface is slightly convex toward a melt near the seed. It gradually became flat and changed to slightly-concave shape as crystal growth proceeded. It is noted that striations are clear in the single crystal region but they become unclear and discontinuous in the polycrystal region. This is because intensity of backscattered electron varies by the channeling effect in polycrystals where crystallographic orientations are different. After 7 mm growth, continuous striations are difficult to be observed but the tendency of gradual curvature change to higher concavity might continue judging from the freezing interface shape at the final stage of the crystal growth. However, it is also said that the concavity at the final stage freezing interface is smaller than that observed in the terrestrially grown samples. Suppression of convection in a melt may contribute to the decrease of concavity at the growth interface. Some cracks are observed clearly in this image adjacent to the Si seed. These cracks might be occurred during cooling process after crystal growth due to thermal expansion coefficient difference between the Si seed and the $Si_{0.5}Ge_{0.5}$ grown crystal. The thermal expansion coefficient of Si is reported to be 3.6×10^{-6} K^{-1} and that of $Si_{0.5}Ge_{0.5}$ is 4.7×10^{-6} K^{-1}at 500 K.[13].

3.5 Growth Rates

Axial growth rates in all space-grown crystals are consistent with those calculated by the one-dimensional TLZ growth model[4]. Observation of striations as shown in **Fig. 6** enabled us to measure axial and radial growth rates more precisely. Therefore, we can compare the experimentally obtained growth rates with theoretically predicted ones by the two-dimensional

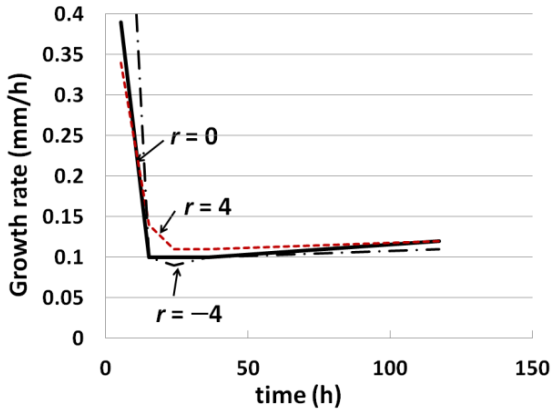

Fig. 7 Axial growth rates along three lines at various *r*, where *r* is the radial distance from the center.

TLZ growth model[5], which are given by eq. (1), where *f*, *t*, C_L, C_S, *D*, *T*, *z*, *r* are interface position, time, liquidus and solidus Ge concentrations at the freezing interface, inter diffusion coefficient between Ge and Si in a liquidus zone, temperature, axial distance and radial distance, respectively.

$$\frac{\partial f}{\partial t} = -\frac{D}{(C_L - C_S)} \frac{\partial C_L}{\partial T} \left(\frac{\partial T}{\partial z} - \frac{\partial T}{\partial r} \frac{\partial f}{\partial r} \right)_L \tag{1}$$

This analysis is now being performed. In the present state, axial growth rate has already been analyzed. According to the two-dimensional TLZ growth model, gradual increase of interface curvature in the process of crystal growth was calculated[5]. In the present experiment, the rate of interface curvature change according as the crystal growth proceeded seemed to be smaller than that of the two-dimensional model prediction. We, therefore, measured growth rates precisely by utilizing intervals of growth striations. Results are shown in **Fig. 7**. In the figure, $t = 0$ is the start of heater translation after 10 h of soaking period. At the start of crystal growth, the growth rate was faster than that of the calculated one using the one-dimensional model[4], but it almost reached to the calculated value after 15 h. The fast growth rate at the initial stage of crystal growth may be due to incomplete dissolution of a Si seed by a Ge melt. In **Fig. 6**, many light flare like patterns are observed at the seed crystal interface and they extend toward the growth direction. These patterns imply inhomogeneous composition at the seed crystal interface, which may cause rapid growth. In the successive growth period between 15 to 36 h, the growth rate was a little smaller than the calculated value. This is because upward heater temperature change was imposed in this period and the melt was often gotten to the unsaturated state. The growth rate gradually increased from 0.10 to 0.12 at the latter part of crystal growth. This is reasonable because heater temperature was lowered than the programmed temperatures in this growth stage and the melt was quickly gotten to the supersaturated state. The growth rate difference between the center and the peripheral region is much important for evaluating our two-dimensional model[5]. However, it is evident that the growth rate along the center line ($r = 0$) and those along the peripheral lines ($r = \pm 4$ mm) are almost equal reflecting the small interface curvature change. These results imply that another growth model except for our two-dimensional model is required but obtained results are favorable for the establishment of radial compositional uniformity. One major candidate of the growth model which describes the radial growth rate difference is considered to be a bundle of one-dimensional capillaries as reported in the result of the second experiment[9]. We are measuring composition along the striations as well as across the striations and analyzing heat and mass transfer during crystal growth. We will accumulate these data and will make clear the controlling factors of interface curvatures and growth rate difference between the center and the peripheral region of the grown crystal.

3.6 Effects of Temperature Gradient

Crystal growth experiments at two different set temperature gradients were performed, namely at 8 °C/cm and 16 °C/cm. It was shown that the growth rate was twice when the temperature gradient was twice. This is consistent with the TLZ growth model. As for the crystal quality, low temperature gradient produced longer single crystal length. This may be related to the degree of constitutional supercooling. In the TLZ growth, the growth rate *R* is dependent on the temperature gradient *G* as described above and cannot be controlled independently. This means that *G/R* is always constant. However, solute concentration in the diffusion boundary layer deviates from the linear approximation when the growth rate is increased and degree of constitutional supercooling increases. This means that lower temperature gradient (lower growth rate) is favorable for the suppression of constitutional supercooling.

4. Summary

Total of four SiGe crystal growth experiments on board the ISS were successfully performed although a little deviation from the expected compositional uniformity due to emissivity change of the cartridge surface oxidation. New information on crystal growth in the diffusion limited regime was obtained. Overall axial growth rate is consistent with that of the one-dimensional TLZ growth model prediction except for initial stage of crystal growth. However, two-dimensional growth rates including radial direction are different from those predicted by our two-

dimensional TLZ growth model. The difference is closely related to the flat freezing interface shape and to the improved radial compositional uniformity. This shows the possibility of large homogeneous SiGe crystal growth. It is expected that obtained results will be utilized in the crystal growth on the ground.

Acknowledgement

We acknowledge all people who engaged in the Hicari experiments such as fabrication of a GHF, preparation of experiment samples, preparatory experiments on the ground, the transportation of cartridges including launching and recovering, operation of the GHF at the mission control center and so on. We also acknowledge crews for handling experiment cartridges.

References

1) H. Stöhr and W. Klemm: Z. Anorg. Chem. **241** (1939) 305.
2) C. D. Thurmond: J. Phys. Chem. **57** (1953) 827.
3) K. Kinoshita, Y. Hanaue, H. Nakamura, S. Yoda, M. Iwai, T. Tsuru, and Y. Muramatsu: J. Crystal Growth, **237** (2002) 1859.
4) H. Nakamura, Y. Hanaue, H. Kato, K. Kinoshita and S. Yoda: J. Crystal Growth, **258** (2003) 49.
5) S. Adachi, K. Kinoshita, M. Takayanagi and H. Miyata: J. Crystal Growth, **334** (2011) 67.
6) K. Kinoshita, Y. Ogata, S. Adachi, S. Yoda, T. Tsuru, H. Miyata and Y. Muramatsu: Ann. New York Acad. Sci., **1077** (2006) 161.
7) K. Kinoshita, Y. Arai, Y. Inatomi, H. Miyata, R. Tanaka, T. Sone, J. Yoshikawa, T. Kihara, H. Shibayama, Y. Kubota, T. Shimaoka, Y. Warashina, K. Sakata, M. Takayanagi and S. Yoda: J. Phys. Conf. Ser. **327** (2011) 012017.
8) K. Kinoshita, Y. Arai, Y. Inatomi, T. Tsukada, S. Adachi, H. Miyata, R. Tanaka, J. Yoshikawa, T. Kihara, H.Tomioka, H. Shibayama, Y. Kubota, Y. Warashina, Y. Sasaki, Y. Ishizuka, Y. Harada, S. Wada, C. Harada, T. Ito, M. Takayanagi and S. Yoda: J. Crystal Growth, **388** (2014) 12.
9) K. Kinoshita, Y. Arai, T. Tsukada, Y. Inatomi, H. Miyata and R. Tanaka: J. Crystal Growth, **417** (2015) 31.
10) K. Kinoshita, Y. Arai, Y. Inatomi, T. Tsukada, H. Miyata, R. Tanaka, J. Yoshikawa, T. Kihara, H. Tomioka, H. Shibayama, Y. Kubota, Y. Warashina, Y. Ishizuka, Y. Harada, S. Wada, T. Ito, N. Nagai, K. Abe, S. Sumioka, M. Takayanagi, and S. Yoda: J. Crystal Growth, **419** (2015) 47.
11) K. Abe, S. Sumioka, K. Sugioka, M. Kubo, T. Tsukada, K. Kinoshita, Y. Arai and Y. Inatomi: J. Crystal Growth, **402** (2014) 71.
12) T. Arai, K. Kinoshita, T. Tsukada, Y. Inatomi, H. Miyata and R. Tanaka, Crystal Growth and Design. (in preparation).
13) H. Kagaya, T. Soma and Y. Kitani: Bussei Kenkyu, **45** (1985) 1 (in Japanese).